

One-pot chemo-enzymatic synthesis and one-step recovery of length-variable long-chain polyphosphates from microalgal biomass

Lin, Yi-Hsuan; Nishikawa, Shota; Jia, Tony Z.; Yeh, Fang-I; Khusnutdinova, Anna; Yakunin, Alexander; Fujishima, Kosuke; Wang, Po-Hsiang

Green Chemistry

Published: 27/10/2023

Peer reviewed version

[Cyswllt i'r cyhoeddiad / Link to publication](#)

Dyfyniad o'r fersiwn a gyhoeddwyd / Citation for published version (APA):

Lin, Y.-H., Nishikawa, S., Jia, T. Z., Yeh, F.-I., Khusnutdinova, A., Yakunin, A., Fujishima, K., & Wang, P.-H. (2023). One-pot chemo-enzymatic synthesis and one-step recovery of length-variable long-chain polyphosphates from microalgal biomass. *Green Chemistry*, (23).

Hawliau Cyffredinol / General rights

Copyright and moral rights for the publications made accessible in the public portal are retained by the authors and/or other copyright owners and it is a condition of accessing publications that users recognise and abide by the legal requirements associated with these rights.

- Users may download and print one copy of any publication from the public portal for the purpose of private study or research.
- You may not further distribute the material or use it for any profit-making activity or commercial gain
- You may freely distribute the URL identifying the publication in the public portal ?

Take down policy

If you believe that this document breaches copyright please contact us providing details, and we will remove access to the work immediately and investigate your claim.

1 **One-pot chemo-enzymatic synthesis and one-step recovery of length-variable**
2 **long-chain polyphosphates from microalgal biomass**

3

4 Yi-Hsuan Lin^{1,†}, Shota Nishikawa^{2,3,†}, Tony Z. Jia^{2,4}, Fang-I Yeh¹, Anna Khusnutdinova⁵,
5 Alexander F. Yakunin⁵, Kosuke Fujishima^{2,6} and Po-Hsiang Wang^{1,7*}

6

7 ¹Graduate Institute of Environmental Engineering, National Central University, Taoyuan, 320 Taiwan (R.O.C)

8 ²Earth-Life Science Institute, Tokyo Institute of Technology, Tokyo 152-8550, Japan

9 ³School of Life Science and Technology, Tokyo Institute of Technology, Tokyo 152-8550, Japan.

10 ⁴Blue Marble Space Institute of Science, Seattle, Washington, USA

11 ⁵Centre for Environmental Biotechnology, School of Natural Sciences, Bangor University, Bangor, LL57 2UW,
12 United Kingdoms

13 ⁶Graduate School of Media and Governance, Keio University, Fujisawa 252-0882, Japan

14 ⁷Department of Chemical and Materials Engineering, National Central University, Taoyuan, 320 Taiwan (R.O.C)

15 [†]These authors contributed equally to this work.

16 *Correspondance: tommy.wang@elsi.jp

17

18

19

20

21

22

23

24

25

26

27

28

29

30

31 **Keywords:** Polyphosphate; microalgae; polyphosphate kinase; one-pot enzyme cascade;
32 bioeconomy; biomass valorization.

33

Abstract

34 Phosphate, an essential ingredient in fertilizers and detergents used daily worldwide, is a
35 finite resource that may be exhausted within 70 years, while improper phosphate waste disposal
36 into aquatic environments will result in eutrophication. Despite some chemical-based methods,
37 biological phosphorus removal using polyphosphate-accumulating organisms, such as microalgae,
38 is a sustainable alternative to reclaim phosphate from wastewater before the wastewater enters
39 aquatic environments, preventing ecosystem damage while recovering the phosphate for industrial
40 use. Moreover, polyphosphates have profound biological functions and biomedical applications,
41 serving as energy stock, drug delivery vesicles, coagulation factors, and antiviral agents depending
42 on the length of the polyphosphate chain, showing inherent value in polyphosphate recovery.
43 However, before this study, there were no sustainable and efficient approaches to synthesizing
44 purified **polyphosphates enriched with different lengths**, which limited industrial and biomedical
45 applications. Here, by leveraging the power of thermodynamic coupling and phase transitions, we
46 established a one-pot, two-step multi-enzyme cascade (comprising creatine kinase and two
47 polyphosphate kinases) to transform heterogeneous polyphosphate in microalgae biomass to
48 insoluble long-chain polyphosphate 1,300-mers, allowing for further purification in **single-step**. In
49 the cascade reactions, introducing creatine as the high-energy P-shuttle enables controlled
50 manipulation of creatine kinase reaction direction *via* pH modulation, effectively circumventing
51 competition between the two polyphosphate kinase-mediated reactions. Finally, we optimized a
52 thermo-digestion approach to transform the polyphosphate 1,300-mers into shorter polyphosphates
53 **enriched with a narrow length range**. **Therefore**, the processes established here create a sustainable
54 P bioeconomy platform to refine microalgal biomass for biotechnological use.

55 Introduction

56 Phosphorus is a key element in the biomass of all living organisms ¹ and is essential for
57 modern agriculture/industry as a component in fertilizer, animal feed, and detergents ². However,
58 the most accessible phosphorus exists in the form of lithosphere apatite minerals and is
59 inaccessible to land-based plants, while worldwide phosphorus demand has been rapidly growing
60 and is expected to exceed supply within 70 years due to rapid global population increase ³. To
61 increase the phosphorus supply, “wet process methods” have been invented to convert unusable
62 inorganic phosphorus into phosphoric acid, a precursor to fertilizers, followed by an introduction
63 to land plants ⁴. However, excessive introduction of soluble phosphorus into aquatic environments
64 is also detrimental ⁵, *e.g.*, phosphorus leakage from agricultural fields, wastewater plants, and
65 household sewage triggers eutrophication in downstream aquatic environments ⁶. Therefore, the
66 sustainable recovery and reuse of phosphorus is urgently needed to sustain the global food chain
67 and other human activities, while preserving aquatic environments.

68 Wastewater is an abundant, widespread phosphorus sink produced by a variety of
69 agricultural and industrial activities. Phosphorus recycling from wastewater would not only
70 prevent further downstream ecological damage but also lead to the development of a sustainable
71 P bioeconomy, where recycled phosphorus can be converted into useful, value-added P-containing
72 materials. In addition to well-established P removal methods, such as adsorption and chemical
73 precipitation ^{7,8}, biological phosphorus removal can occur through polyphosphate-accumulating
74 organisms (PAOs) uptaking phosphorus from wastewater and accumulating the phosphorus in the
75 form of inorganic polyphosphate (polyP) ⁹⁻¹²; the accumulated polyP can subsequently be

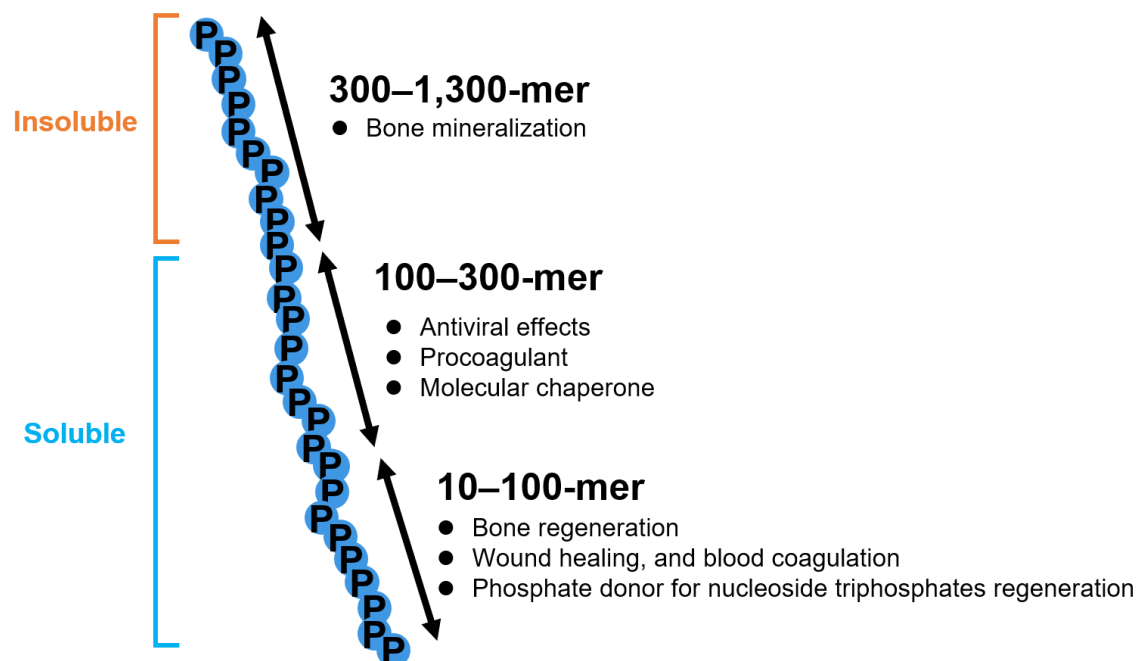
76 extracted from microalgal cells for downstream application ¹³. These examples suggest that
77 biological phosphorus removal systems are eco-friendly and cost-effective, making them good
78 candidates for developing the sustainable P bioeconomy.

79 PolyP has numerous biological functions and biomedical applications, which vary
80 depending on chain length (**Figure 1**) ^{14,15}; short/medium-chain polyP (10–100-mer) promotes
81 bone regeneration ¹⁶, wound healing ^{17,18}, and blood coagulation ^{19,20}, while long-chain polyP
82 (100–1,000-mer) are less soluble (>300-mer is insoluble)²¹ and can be used as biomolecule-
83 carrying microdroplets that exhibit antiviral properties ^{22–24} or as molecular chaperones ²⁵.
84 Traditionally, phosphate glass, composed of polydisperse polyP, is synthesized by heating
85 phosphoric acid at high temperatures (>700°C) ²⁶. The chemically synthesized polyP is then
86 partially hydrolyzed by the alkaline treatment and separated by length *via* liquid chromatography
87 or fractional precipitation using organic solvents, which are resource and time-intensive ²⁷, along
88 with low yields of polyP of each specific length. Similar to chemical methods, polyP purified from
89 microalgal systems is also polydisperse ²⁸, which also requires separation and harvesting for
90 downstream use. Thus, for microalgal phosphate removal systems to be included within the
91 sustainable P bioeconomy, the development of a sustainable method to produce length-variable
92 polyP of higher homogeneity is necessary.

93 As polyP is ubiquitous in biology and because polyP function varies depending on chain
94 length, organisms must harbor some biochemical mechanisms to produce polyP of a specific
95 length to achieve their physiological goals. In prokaryotes, the biosynthesis and utilization of polyP
96 are primarily mediated by polyP kinases (PPKs) with the two main families represented by PPK1s

97 and PPK2s, which catalyze the reversible transfer of phosphate between polyP and nucleotides ²⁹.
98 Recent phylogenetic analysis has identified three subtypes of PPK2s (class I, II, and III) ^{30,31}; class
99 I and II PPK2s catalyze the polyP-driven phosphorylation of either NDP or NMP, respectively,
100 while class III PPK2s can phosphorylate both NDP and NMP, enabling direct NTP production
101 from NMP ³². Class I and II PPK2s have been used for *in vitro* biosynthesis of acetone ³³, aldehyde
102 ³⁴, and thiamine phosphates ³⁵ as well as biocatalytic regeneration of S-adenosyl-L-methionine ³⁶,
103 while class III PPK2s have been used for cell-free protein synthesis and *in vitro* biocatalytic
104 reactions that simultaneously require regeneration of both ATP and GTP ³⁷. In the PPK2-mediated
105 A(G)TP regeneration system, long-chain polyP (100-mer), as opposed to short-chain polyP at the
106 same molar content of total orthophosphate, can significantly enhance cell-free protein yield.

107 Inspired by biology, we aimed to develop a sustainable mechanism to synthesize length-
108 variable long-chain polyP. Given that *Cytophaga* PPK2 can use polydisperse polyP to
109 phosphorylate ADP to ATP, while *Ralstonia eutropha* PPK2c can catalyze the direct synthesis of
110 insoluble long-chain polyP (length undetermined) from ATP without a priming short-chain polyP
111 ^{38,39}, we harnessed these two PPK2 enzymes in tandem to convert polydisperse polyP in
112 wastewater microalgae biomass into insoluble long-chain polyP 1,300-mer with creatine as the P-
113 shuttle (**Table 1**). The insoluble long-chain polyP 1,300-mer then can be purified by a simple one-
114 step filtration (phase transition), followed by non-enzymatic degradation to yield length-variable
115 polyP enriched with varying shorter lengths.



116

117 **Figure 1. Functional diversity of polyphosphates of different lengths.**

118

119

120 **Experimental section**

121 For full experimental details please refer to the ESI. Unless specified otherwise, chemicals and
 122 reagents are purchased from Sigma-Aldrich (St. Louis, MO, USA). **Enzyme kinetics and sources**
 123 **of the recombinant enzymes used in this study are provided in Tables S1 and S2 in**
 124 **Supplementary Information. Sodium dodecyl sulfate-polyacrylamide gel electrophoresis (SDS-**
 125 **PAGE) gel images of the purified recombinant enzymes; HPLC chromatograms of creatine**
 126 **phosphate and creatine; standard curves of NAD(P)H, creatine phosphate, polyphosphate, and**

127 ATP; and the geographical coordinate of the P-rich wastewater-sampling site are available in

128 **Appendix.**

129 *Quantification of polyP using the toluidine blue O (TBO) method*

130 PolyP was quantified by a metachromatic assay with the TBO method using commercial polyP
131 (sodium polyP (~25-mer); Sigma-Aldrich) as a standard. The TBO method is based on the
132 concentration-dependent decrease in $\lambda_{630\text{ nm}}$ by the metachromatic reaction of TBO with polyP⁴⁰.
133 Briefly, sample solution (5 μL) was mixed with TBO assay solution (250 μL ; 15 $\mu\text{g}/\text{mL}$) and acetic
134 acid (0.1 N) at room temperature⁴¹. Then, $\lambda_{630\text{ nm}}$ was measured for the TBO-treated sample in a
135 microplate spectrophotometer for 10 min (Molecular Devices/Spectra Max® iD3, San Jose, CA,
136 USA). The $\lambda_{630\text{ nm}}$ was later converted into polyP concentration based on standard curves derived
137 from the different commercial sodium polyP standard concentrations. The standard curves of
138 polyP concentrations are available in the **Appendix**.

139 *Microalgae cultivation under nitrogen-deficient conditions*

140 Microalgae *Chlorella vulgaris* (*C. vulgaris*) was purchased from the Bioresource Collection and
141 Research Center (Hsinchu, Taiwan), which was cultivated in heat-sterilized wastewater collected
142 from the discharge of a local piggery wastewater treatment plant with continuous daylight
143 exposure (**Appendix**). *C. vulgaris* was cultivated in 2 L Erlenmeyer flasks containing the sterilized
144 wastewater (1 L; pH adjusted to neutral) at room temperature with continuous shaking (200 rpm)
145 for aeration and to prevent microalgae from sticking to the bottom of the flask as previously
146 described⁴².

147

148 ***Epifluorescence microscopic detection of polyP***

149 PolyP was detected by epifluorescence microscopy as previously described³⁸. Briefly, polyP
150 granules were stained with DAPI (4',6-diamidino-2-phenylindole) (0.1 mg/mL in distilled H₂O)
151 for at least 10 min and the stained granules were visualized by epifluorescence microscopy on an
152 oil objective at 1,000 x magnification (ZEISS/AXIOSKOP 2, Oberkochen, Germany).

153 ***In vivo polyP visualization using TBO staining***

154 *C. vulgaris* cells were air-dried and heat-fixed on a glass slide (76 × 26 mm; Thickness 1.2–1.5
155 mm). Intracellular polyP granules were then stained with TBO (15 mg/L) for 10 min by
156 submerging the whole glass slide (containing the fixed cells) into TBO solution. The slide was
157 then gently washed with double distilled H₂O, followed by air drying for 15 min and subsequent
158 observation by an optical microscope at 100 x magnification (Olympus CX21FS1, Shinjuku,
159 Tokyo, Japan).

160 ***C. vulgaris cell lysis and partial polyP purification***

161 The *C. vulgaris* cells were disrupted and partially purified as previously described⁴⁰. *C. vulgaris*
162 biomass was collected by centrifugation at 4,430 × g for 10 min at room temperature and then
163 resuspended in buffer (HEPES-K (pH 7.0; 20 mM), KCl (0.15 M), and ethylenediaminetetraacetic
164 acid (EDTA) (5 mM)) at a pellet to buffer ratio of 1:3. The cells were lysed *via* ultrasonication for
165 20 min (3 s on and 3 s off) and the cell-lysate containing polyP was subsequently incubated at
166 100°C for 10 min, followed by centrifugation at 8,000 × g for 3 min at room temperature to separate
167 the cell debris from the supernatant containing the polydisperse polyP. The polyP concentration
168 within the supernatant and the initial microalgal wastewater were quantified by the TBO method

169 (see above). The supernatant containing polyP was stored at -80°C for further use in subsequent
170 experiments.

171 *ATP regeneration using polydisperse microalgal polyP*

172 Polydisperse polyP in the microalgal cell-lysate was used for ATP regeneration using the
173 *Cytophaga* PPK2. In the phospho-transfer reaction, the theoretical product is ATP and polyP with
174 one less unit in the chain ($\text{polyP}_{(n)} + \text{ADP} \rightarrow \text{polyP}_{(n-1)} + \text{ATP}$). To measure the reaction kinetics for
175 stoichiometric analysis, ATP production was monitored by both (i) the time-dependent
176 consumption of polyP using the TBO method (see above) and (ii) the hexokinase/glucose-6-
177 phosphate dehydrogenase (Roche, Basel, Switzerland)-coupled NADP^+ reduction process ($\lambda_{340\text{ nm}}$)
178 as described previously³⁷. In the coupled HK/G6PD enzyme cascade, glucose is first converted
179 into glucose-6-phosphate by HK using one ATP, which is then converted into dehydro-glucose-6-
180 phosphate, along with the reduction of one NADP^+ to produce one NADPH, which can be
181 observed through $\lambda_{340\text{ nm}}$. The reaction mixtures (200 μL) contained Tris-HCl (pH 7.0; 100 mM),
182 Mg^{2+} (10 mM), microalgal polyP (1.5–10 mM), adenosine (1–3 mM), and *Cytophaga* PPK2 (0.08
183 mg/mL). The reaction was initiated by the addition of PPK2 and the ATP production was
184 monitored at 37°C for 10 min by measuring the ATP-dependent NADP^+ reduction through the
185 increase in $\lambda_{340\text{ nm}}$.

186 *Enzymatic synthesis of creatine phosphate from polydisperse polyP in microalgal cell-lysate*

187 A two-enzyme cascade comprising *Cytophaga* PPK2 and rabbit creatine kinase (CK) (Sigma-
188 Aldrich) was applied to sequentially convert the microalgal polyP into creatine phosphate *via* ATP.
189 The optimized reaction mixtures (200 μL) contained Tris-HCl (pH 9.0; 0.1 M), MgSO_4 (10 mM),
190 microalgal polyP (10 mM), creatine (50 mM), ATP (1 mM), N-acetyl-L-cysteine (2 mM),

191 *Cytophaga* PPK2 (0.3 mg/mL), and CK (0.03 mg/mL); different conditions, including pH 8.0, 5
192 mM and 15 mM MgSO₄, and 10–40 mM creatine were also tested, but the reported reaction
193 conditions are the optimized conditions (10 mM Mg²⁺, 5 mM microalgal polyP, and 50 mM
194 creatine at pH 9.0 in Tris buffer) for the greatest amount of creatine phosphate conversion (~4.75
195 mM; 95% yield), which were used for all subsequent experiments. The reaction was initiated by
196 the addition of *Cytophaga* PPK2 and CK, and the formation of creatine phosphate was monitored
197 at 30°C for 30 min by the consumption of the microalgal polyP using the TBO method (see above)
198 as well as HPLC analysis.

199 ***Enzymatic synthesis of insoluble polyP 1,300-mer***

200 Another two-enzyme cascade comprising *Ralstonia* PPK2c (polyP-synthesizing) and rabbit CK
201 was used to sequentially convert creatine phosphate into homogeneous polyP 1,300-mer *via* ATP.
202 The formation of the polyP 1,300-mer was monitored by the TBO method (see above). The
203 reaction mixtures (200 µL) contained (HEPES-K (pH 7.0; 90 mM), Tris-HCl (pH 7.0; 10 mM),
204 MgSO₄ (10 mM), creatine phosphate (5 mM), ATP (3.5 mM), PPK2c (0.5 mg/mL), and CK (0.1
205 mg/mL); different ATP concentrations (1–5 mM) were also tested, but the reported reaction
206 conditions are the optimized conditions used for all subsequent experiments. The reaction was
207 initiated by the addition of CK and *Ralstonia* PPK2c at 30°C and the formation of the polyP 1,300-
208 mer was monitored *via* the time-dependent decrease in λ_{630 nm} using the TBO method.

209 ***Degradation of insoluble polyP 1,300-mer by non-enzymatic hydrolysis***

210 The synthesized polyP 1,300-mer in the microalgal cell-lysate was collected by filtration using a
211 0.45-µm MF-Millipore® membrane filter paper (Burlington, Massachusetts, USA) along with a
212 vacuum pump. The remainder was washed by ddH₂O until the intensity of λ_{265 nm} (indicative of

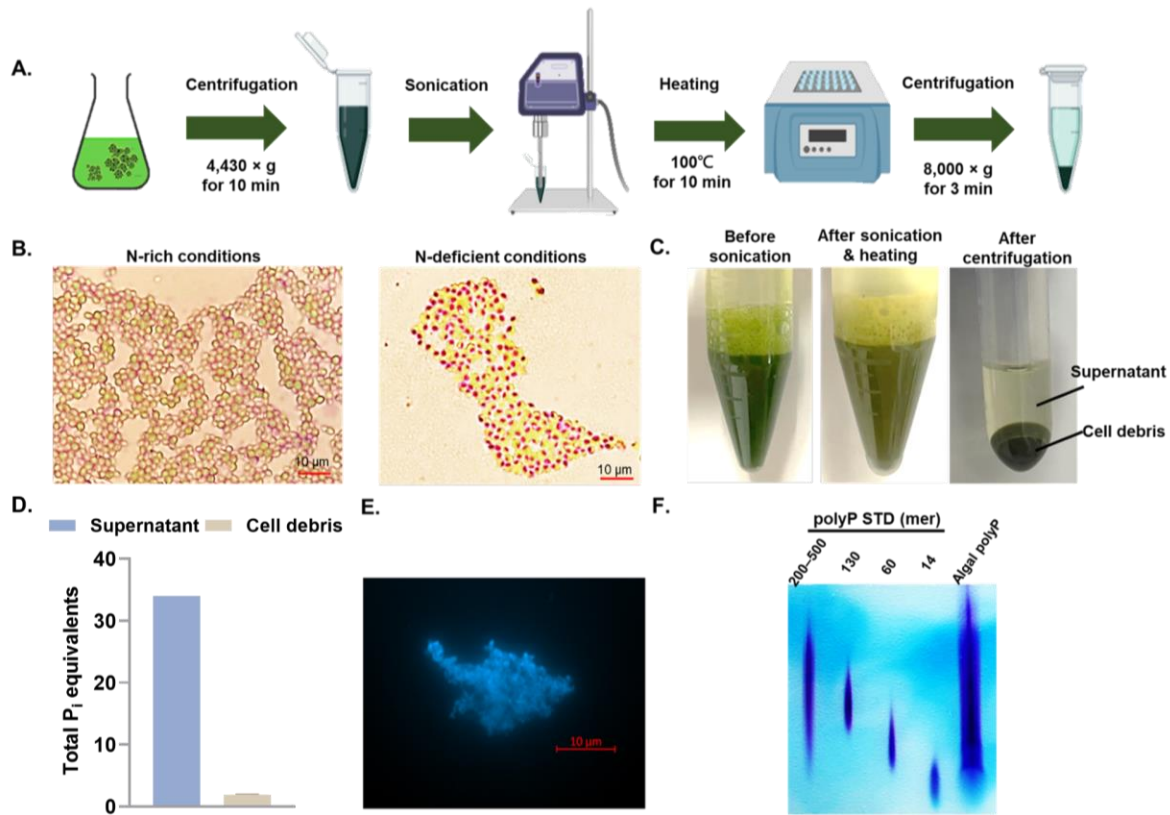
213 N(M/D/T)P) and $\lambda_{280\text{ nm}}$ (indicative of protein/polypeptide) of the flowthrough decreased to
214 background levels. After resuspension of the reaction by adding 300 μL HEPES-K buffer (25 mM;
215 pH 7.5), the reaction mixture (MgSO_4 (5 mM), EDTA (5 mM), and polyP 1,300-mer (5 mM)) was
216 subjected to time-dependent hydrolysis at 95°C.

217

218 **Results**

219 **Polydisperse polyP extraction from wastewater microalgal biomass**

220 To develop the sustainable P bioeconomy process, we selected wastewater discharge
221 samples collected from a local piggery as a substrate for microalgae cultivation and polyP
222 production (**Figure 2A**). *Chlorella vulgaris* was cultivated in heat-sterilized wastewater discharge
223 under nitrogen-deficient conditions to induce phosphorus assimilation in the form of polyP⁴³.
224 After cultivation, TBO was used to live-stain the microalgal cells and *in vivo* visualize the
225 accumulation of small purple-stained particles within the cells, approximately 1 μm in diameter,
226 which were likely highly enriched in polyP (**Figure 2B**). The polyP-accumulating microalgal
227 biomass was then collected by centrifugation and lysed by sonication in an ice bath, followed by
228 heating at 100°C with the EDTA to prevent non-enzymatic polyP degradation (**Figures 2C and**
229 **S1AB**). The heating step significantly enhanced the extraction efficiency and prevented enzymatic
230 polyP degradation, resulting in microalgal cell-lysates containing up to 35 mM polyP (**Figure 2D**).
231 Thus, microalgal polyP in the form of heterogeneous solid particle-like structures (**Figure 2E**) can
232 be collected using simple cultivation and extraction. Moreover, the cell-lysate polyP appeared to
233 be polydisperse in length (**Figure 2F**).



235

236 **Figure 2. Microalgae cultivation and partial fractionation of the accumulated polyphosphate**
 237 **(polyP).** (A) The overall scheme for producing polydisperse microalgal polyP. (B) PolyP
 238 accumulation in *Chlorella vulgaris* cultivated in sterilized wastewater under nitrogen-deficient
 239 conditions. The intracellular polyP was visualized *in vivo* by TBO staining and analyzed by optical
 240 microscopy. (C) Production of the polyP-rich cell-lysate (supernatant) from microalgal biomass
 241 *via* sonication, heating, and centrifugation. (D) The soluble polyP concentrations (shown in total
 242 P_i equivalents) in the supernatant and the cell debris (measured by the TBO assay). Error bars
 243 represent the standard deviation from three experimental replicates. (E-F) DAPI-stained
 244 epifluorescent microscopy analysis (E) and TBE-Urea polyacrylamide gel electrophoresis (6%,
 245 w/v) analysis (F) of the granular polydisperse polyP aggregates.

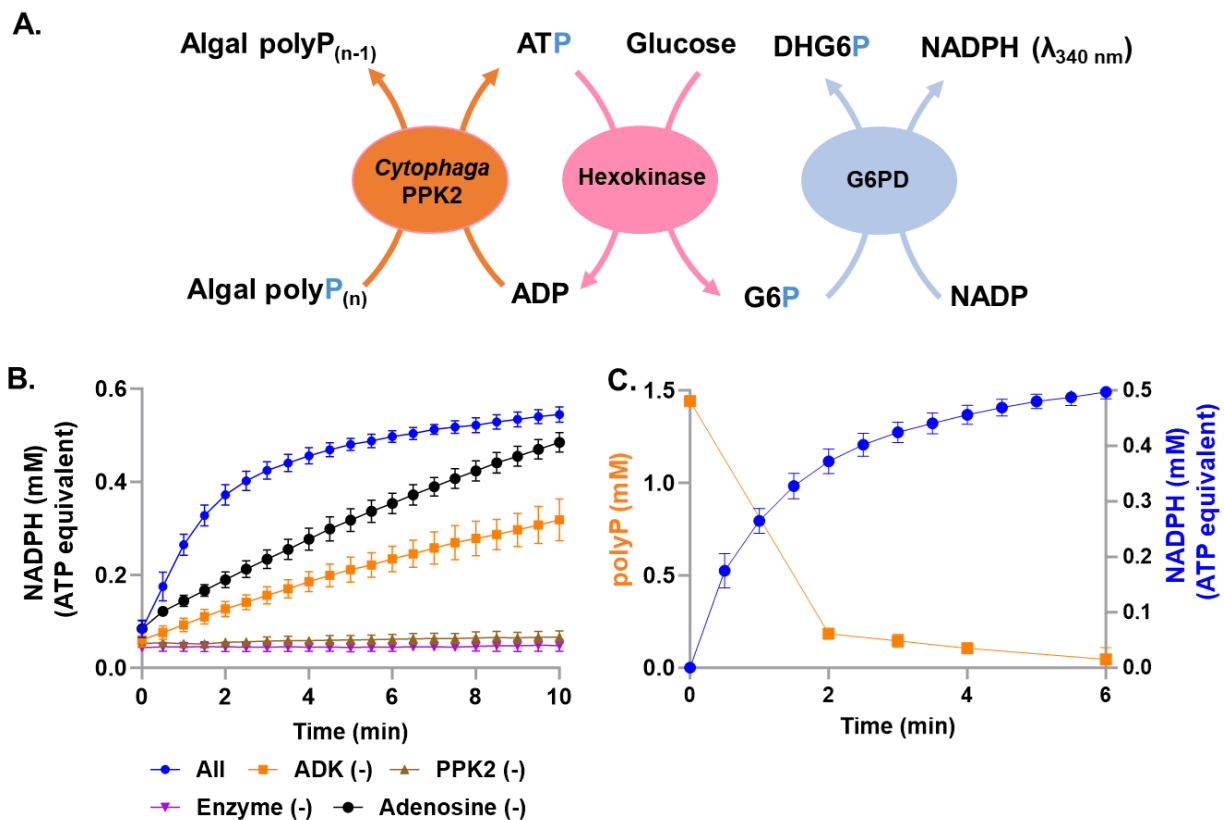
246

247

248

Polydisperse microalgal polyP as P-donor for PPK2-mediated ATP regeneration

249 The next step for the proposed sustainable P bioeconomy was to convert the polydisperse
250 microalgal polyP to another P-containing molecule (creatine phosphate) for the downstream
251 synthesis of homogeneous long-chain polyP. However, the prerequisite of this step is that the
252 microalgal cell-lysate polyP can serve as the substrate of *Cytophaga* PPK2, similar to the case with
253 commercial polyP 25-mers (Figure S2), so that the high-energy phosphate can be completely
254 transferred to the downstream P-carrier. To measure the reaction kinetics to confirm complete P
255 transfer from polyP to produce ATP, we coupled the *Cytophaga* PPK2-mediated ATP production
256 process to an NADP reduction process driven by an enzyme cascade consisting of hexokinase
257 (HK) and glucose-6-phosphate dehydrogenase (G6PD) (Figure 3A). Upon incorporation of the
258 HK/G6PD cascade to the *Cytophaga* PPK2-mediated ATP production process, we observed
259 NADPH accumulation over time upon progression of this reaction in the microalgal cell-lysate
260 (Figure 3B); stoichiometric analysis also confirmed that NADPH production (*i.e.*, ATP
261 regenerated) is equivalent to polyP consumption, suggesting that all high-energy phosphate
262 contained within polyP was transferred fully to produce ATP (Figure 3C).



263
264

265 **Figure 3. *Cytophaga* PPK2-based ATP regeneration using polydisperse polyP in microalgal**
 266 **cell-lysate.** (A) Schematic diagram showing the enzymatic cascade of the *Cytophaga* class III
 267 PPK2 and HK-G6PD-coupled NADPH production assay. HK; hexokinase, G6PD; glucose-6-
 268 phosphate dehydrogenase, DHG6P; dehydroglucose-6-phosphate. (B) PolyP-based ATP
 269 regeneration monitored by ATP-dependent NADPH production ($\lambda_{340\text{ nm}}$) using G6PD-HK. (C)
 270 Stoichiometric analysis of *Cytophaga* PPK2-dependent polyP consumption and ATP-dependent
 271 NADPH production by HK-G6PD. The concentrations of the consumed polyP and produced
 272 NADPH were monitored through the TBO assay and at $\lambda_{340\text{ nm}}$, respectively. The error bars
 273 represent the range and the data points represent the average from two independent experimental
 274 replicates.

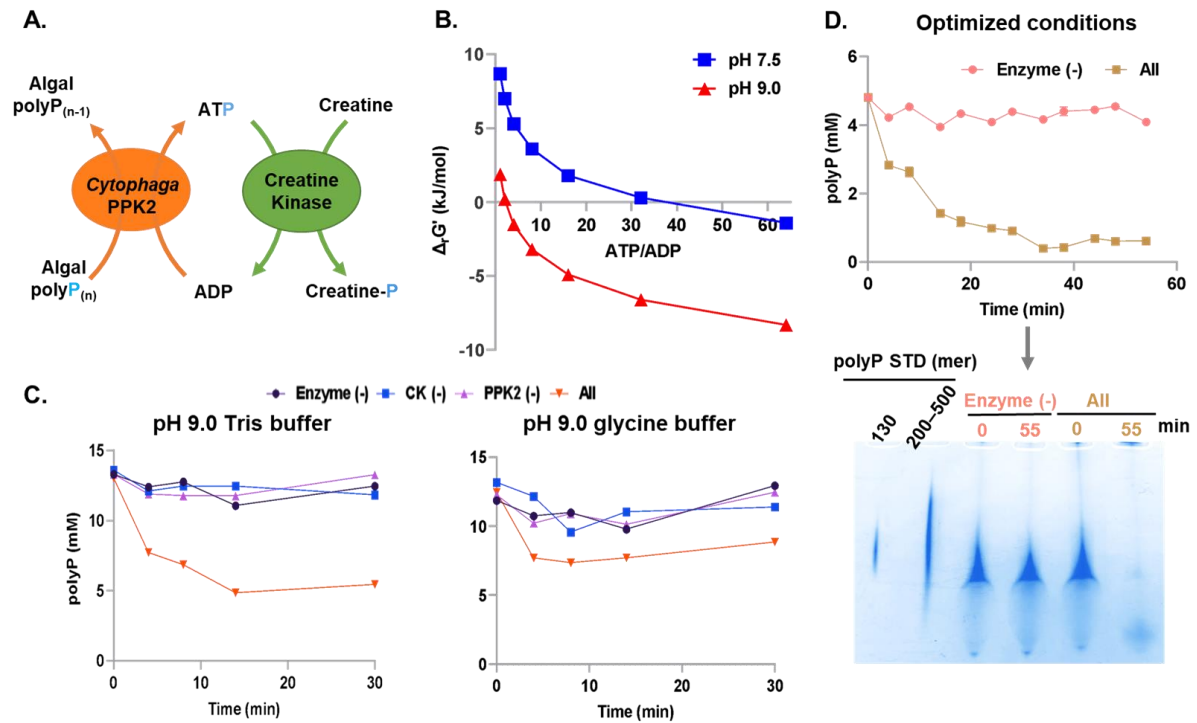
275

276

277

278 **Stepwise conversion of polydisperse microalgal polyP into insoluble long-chain polyP 1,300-**
279 **mer**

280 We then chose creatine phosphate as the P-carrier for downstream synthesis of insoluble
281 long-chain polyP (**Figure 4A; Table 1**), as eQuilibrator-based free energy calculations suggest
282 that CK-mediated phospho-transfer from ATP to creatine is thermodynamically favorable at basic
283 pH (**Figures 4B and S3A**)⁴⁴. Given the previous demonstration that P from microalgal polyP can
284 be fully converted to ATP, complete phospho-transfer from the polydisperse polyP to creatine *via*
285 ATP in the microalgal cell-lysate is plausible. On the other hand, the CK-mediated phospho-
286 transfer from creatine phosphate to ADP (the reverse reaction) is thermodynamically favorable at
287 neutral pH (**Figure S3B**). Therefore, by modulating the pH of the microalgal cell-lysate, we
288 attempted to first convert the polydisperse polyP and creatine into creatine phosphate *via* ATP
289 ($\text{polyP}_{(n)} + \text{creatine} \rightarrow \text{polyP}_{(n-1)} + \text{creatine phosphate}$) using polyP-consuming *Cytophaga* PPK2
290 and CK at basic pH, and later convert creatine phosphate back into long-chain **polyP and** creatine
291 using CK and polyP-synthesizing *Ralstonia* PPK2c *via* ATP at neutral pH ($\text{polyP}_{(n)} + \text{creatine}$
292 $\text{phosphate} \rightarrow \text{polyP}_{(n+1)} + \text{creatine}$). Using free energy calculations as a guide (**Figure S3**), we
293 optimized the conditions of the two-enzyme PPK2/CK cascade (**Figure 4A**). The greatest polyP
294 consumption and creatine phosphate production were observed with 10 mM Mg^{2+} at pH 9.0
295 (**Figures 4C and S4A–E**), while 5 mM microalgal polyP also resulted in nearly complete polyP
296 consumption (**Figure 4D**).



297

298 **Figure 4. Conversion of polydisperse microalgal polyP into creatine phosphate via ATP by**
 299 **the enzymatic cascade comprising CK and *Cytophaga* PPK2.** (A) Schematic diagram showing
 300 the PPK2-CK enzyme cascade. (B) eQuilibrator-based thermodynamic calculations of creatine
 301 phosphorylation at circumneutral (pH 7.5) or alkaline (pH 9.0) pH. (C) Time-dependent creatine
 302 phosphate production by the PPK2-CK cascade in Tris-HCl or glycine buffer at pH 9.0. The
 303 production of creatine phosphate was monitored by the consumption of the polyP via TBO assay.
 304 (D) Time-dependent creatine phosphate production by the PPK2-CK cascade under optimized
 305 conditions (Tris-HCl (pH 9.0), Mg²⁺ (10 mM), creatine (50 mM), and microalgal polyP (5 mM)).
 306 The reactions were conducted with and without *Cytophaga* PPK2. The nearly complete
 307 consumption of polyP was verified via quantitative TBO measurements (top) from TBE-Urea
 308 polyacrylamide gel electrophoresis analysis (bottom).

309

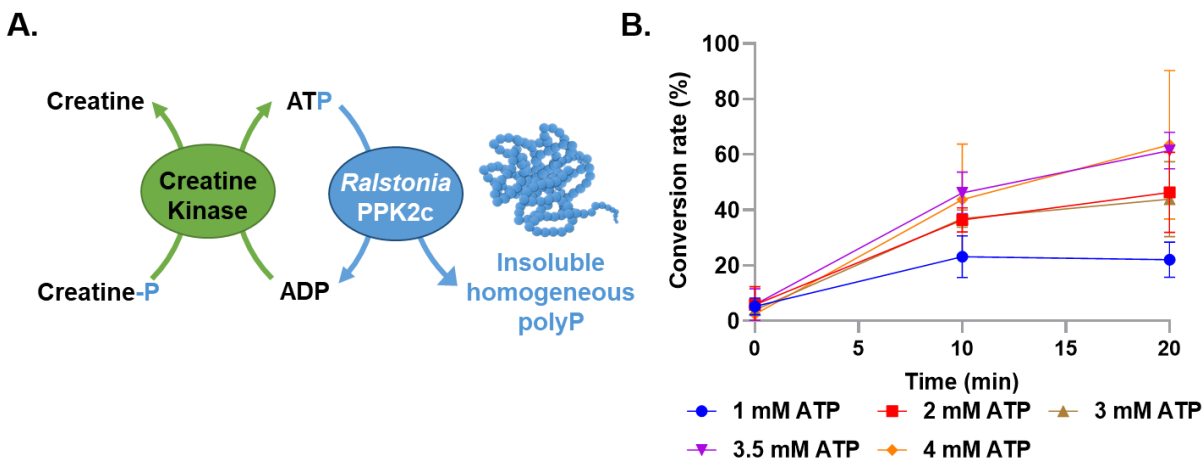
310

311 Next, we sought conditions to transfer the high-energy phosphate from creatine phosphate
312 to build a growing polyP chain. Thus, we then applied a two-enzyme cascade containing CK and
313 *Ralstonia* PPK2c in HEPES-K at neutral pH with ATP as the P shuttle (pH 7.0); the high-energy
314 phosphate from creatine phosphate is transferred to ADP via CK (regenerating ATP), while the
315 *Ralstonia* PPK2c transfers the high-energy phosphate on the regenerated ATP onto a growing
316 polyP chain (Figure 5A). After optimization through a combination of free energy calculations
317 and experiments, efficient conversion of the creatine phosphate into polyP via the CK/PPK2c
318 cascade was successfully demonstrated with the initial addition of 3.5 mM ATP (Figures 5B and
319 S3B). In the absence of creatine phosphate (but with added ATP), nearly no long-chain polyP was
320 produced, suggesting the importance of creatine phosphate to drive the aforementioned exergonic
321 phospho-transfer (thermodynamic coupling) (Figure S5).

322

323

324



325

326 **Figure 5. Conversion of creatine phosphate into homogeneous insoluble long-chain polyP via**
327 **ATP by the enzymatic cascade comprising CK and *Ralstonia* PPK2c.** (A) Schematic diagram
328 showing the two-enzyme cascade comprising CK and *Ralstonia* PPK2c for homogeneous
329 insoluble long-chain polyP production. (B) Time-dependent long-chain polyP production by the
330 CK-PPK2c cascade in HEPES-K buffer (pH 7.5) with varying ATP concentrations. Error bars
331 represent the standard deviation and the data points represent the mean from three independent
332 experimental replicates.

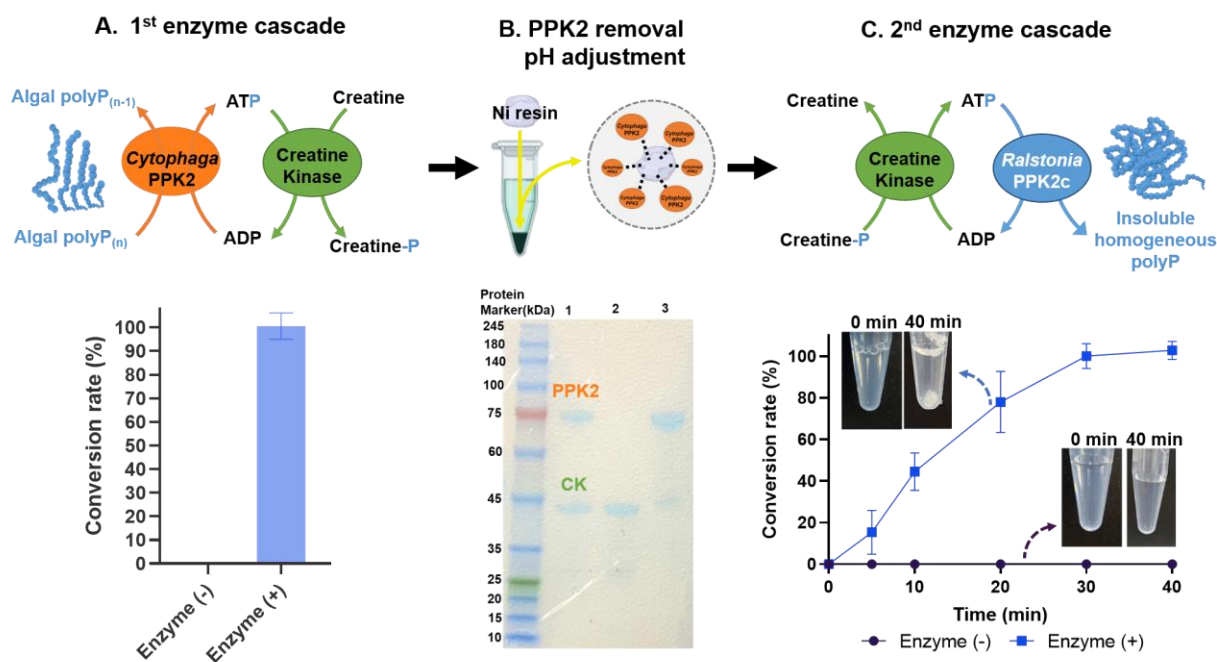
333

334 **One-pot enzymatic synthesis and one-step recovery of insoluble long-chain polyP 1,300-mer**
335 **from polydisperse polyP**

336 Next, given that both enzymatic cascades (*Cytophaga* PPK2-CK and CK-*Ralstonia*
337 PPK2c) were shown separately to be effective to convert the polydisperse microalgal polyP into
338 long-chain polyP via creatine phosphate, we then sought to perform the entire reaction in a one-
339 pot, two-step fashion for greater throughput and scalability. Specifically, we first applied the
340 creatine phosphate-producing cascade (*Cytophaga* PPK2-CK) at pH 9.0 (Figure 6A), followed by
341 the removal of *Cytophaga* PPK2 and adjustment of the reaction pH to neutral (Figure 6B) and
342 addition of *Ralstonia* PPK2c to transform the produced creatine phosphate to ATP and then to the
343 long-chain polyP (Figure 6C). However, our experimental analysis revealed that the two cascades
344 require completely different buffer systems at the required pH range (pH 7.0–9.0) to be active.
345 Thus, we reasoned that a mixture of buffers amenable to each cascade at an intermediate pH may
346 facilitate both cascades in the same pot, albeit possibly with sub-optimal efficacy for either or both
347 cascades. Among all conditions tested, a HEPES-K:Tris-HCl ratio of 8:1 resulted in the greatest
348 long-chain polyP production (Figures S6A–E). In parallel, we observed a nearly complete
349 conversion of the creatine phosphate into long-chain polyP and creatine by the CK-*Ralstonia*

350 PPK2c cascade under the same assay conditions but in the HEPES buffer (Table 2), suggesting
 351 that the mixed buffer is indeed sub-optimal for the CK-*Ralstonia* PPK2c cascade. However,
 352 considering that the *Cytophaga* PPK2-CK cascade requires completely different conditions, the
 353 mixed buffer conditions can still produce long-chain polyP at a high yield (90%) through a one-
 354 pot, two-step process.

355



356

357 **Figure 6. One-pot, two-step enzymatic synthesis of homogeneous insoluble long-chain polyP**
 358 **from polydisperse microalgal polyP.** (A) Conversion of polydisperse microalgal polyP into
 359 creatine phosphate via the *Cytophaga* PPK2-CK cascade. (B) The removal of His-tagged
 360 *Cytophaga* PPK2 from the microalgal cell-lysate (verified by SDS-PAGE) using the Ni-chelating
 361 resin. 1: the cell-lysate with both *Cytophaga* PPK2 and CK; 2: the cell-lysate after *Cytophaga*
 362 PPK2 removal by a Ni-chelating resin; 3: the elution of the Ni-chelating resin used for *Cytophaga*
 363 PPK2 removal. A trace amount of CK was also co-eluted. (C) Conversion of creatine phosphate
 364 into homogeneous insoluble long-chain polyP solids via the CK-*Ralstonia* PPK2c cascade. The

365 conversion rates of the insoluble long-chain polyP synthesis reaction with the mixed buffer system
366 were calculated at different time points. The reactions were conducted with and without *Ralstonia*
367 PPK2c. Error bars represent the standard deviation and the data points represent the mean from
368 three independent experimental replicates.

369

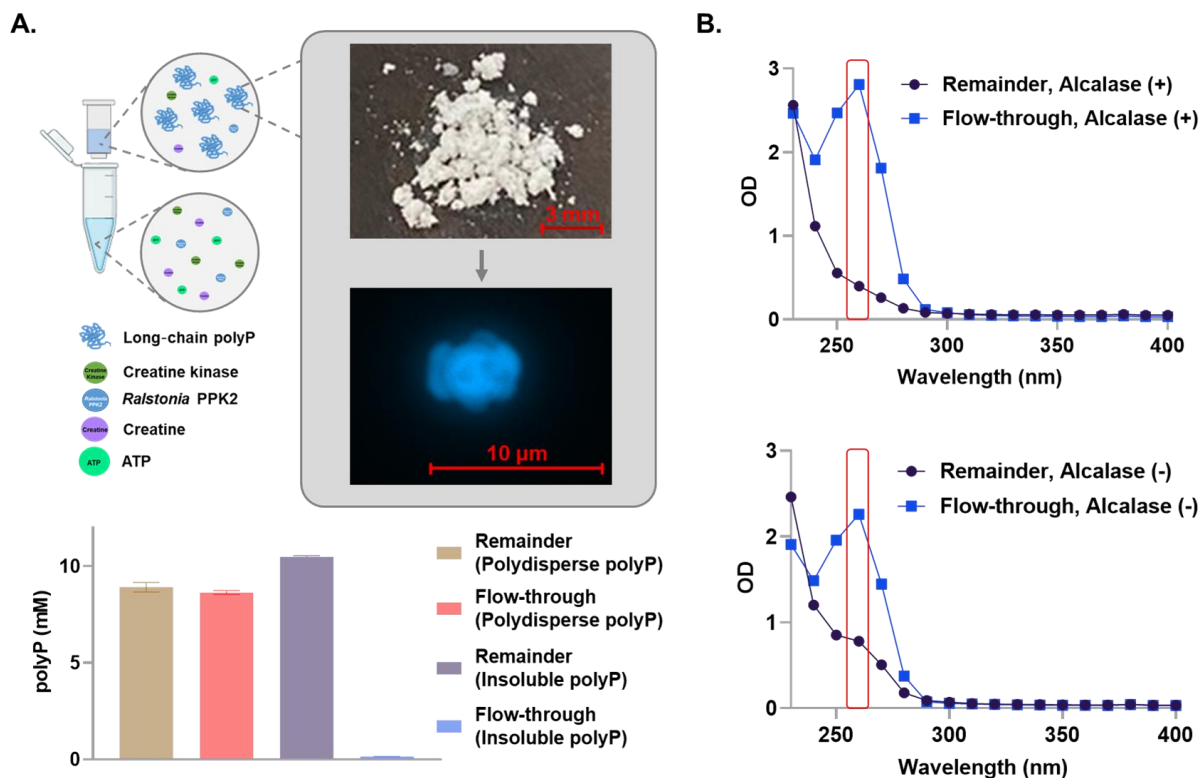
370

371

372 We also observed insoluble material produced after the one-pot, two-step enzymatic
373 cascade (**Figure 6C**). As polyP >300-mer is generally insoluble, which we conjectured was the
374 chain length of the polyP product. After filtration using a 100-kDa cutoff centrifugal filters, the
375 polyP products appeared to be all “ultra” long-chain polyP (>100-kDa or >1,000-mer), which was
376 highly homogeneous and in the 1,300-mer unit range (**Figure 7A and S7AB**). This is in contrast
377 to the polydisperse polyP in microalgal cell-lysate before the enzymatic catalysis, which has
378 roughly equal concentrations of polyP of sizes larger and smaller than 100 kDa (**Figure 2F**). Prior
379 to this study, long-chain polyP 700-mer was referred to as “super long-chain” polyP; however, our
380 enzymatically synthesized homogeneous polyP product is nearly twice as long compared to the
381 longest commercially available polyP.

382 Although homogeneous long-chain polyP has been produced *via* our one-pot, two-step
383 enzymatic cascades, the product could potentially contain some byproducts or contaminants, such
384 as nucleic acids and peptides, that would inhibit downstream use or processing for industrial
385 purposes. We thus further subjected the microalgal cell-lysate containing the polyP 1,300-mer
386 product to a protease treatment and filtration by a 0.45- μ m filter for polyP purification.

387 Consistently, ATP and proteins (indicated by $\lambda_{260-280\text{ nm}}$) were nearly completely removed (Figures
 388 7B and S7C; Table 2), suggesting effective purification of the polyP 1,300-mer product. After
 389 filtration, we then dried the remainder, which resulted in a white powder that fluoresced after
 390 DAPI-staining, confirming its composition to be of polyP (Figure 7A).



391
 392 **Figure 7. Purification of long-chain polyP using a membrane filter after the protease**
 393 **digestion.** (A) The solutions containing the polydisperse microalgal polyP or the insoluble
 394 homogeneous long-chain polyP obtained from the one-pot, two-step enzymatic cascades were
 395 subjected to filtration through a 100-kDa filter. PolyP concentrations in the remainder and flow-
 396 through fractions were quantified by the TBO assay. (B) Removal of small molecules (ATP,
 397 creatine, and salts) and proteins from the remainder fraction (verified by UV-Vis analysis). The
 398 reaction mixture containing insoluble long-chain polyP was subjected to filtration before and after
 399 the proteolysis treatment.

400
401
402
403
404
405
406
407
408
409
410
411
412
413
414
415
416
417
418
419
420

Non-enzymatic production and application of length-variable polyphosphates from homogeneous long-chain polyP

While the goal of this study was to convert polydisperse polyP in wastewater microalgae biomass into insoluble and homogeneous long-chain polyP, we next wondered whether the developed process could lead to more value-added products aside from the polyP 1,300-mer. As mentioned previously, polyPs of different lengths have different functional properties, and the ability to acquire polyPs of different lengths is of particular value. Before this study, industrial production methods for polyP of different chain lengths were time-, resource-, cost-, and organic waste-intensive. Thus, to produce a shorter homogeneous polyP, we first subjected the polyP 1,300-mer to enzymatic treatment by exopolyphosphatase (PPX)⁴⁵. However, rather than the polyP product length decreasing over time, the polyP concentration instead decreased over time (Figure S8A). Moreover, the treatment of polyP 1,300-mer with polyP-consuming *Cytophaga* PPK2 also resulted in a similar result (Figure S8B). We attribute this to the fact that PPX and *Cytophaga* PPK2 likely degrade single polyP chains fully before moving on to the next chain. Therefore, such an enzymatic degradation strategy was not amenable to our goals.

We thus decided to search for a non-enzymatic strategy for polyP length shortening that did not degrade single polyP chains fully. As Mg²⁺ is a known catalyst for non-enzymatic ATP

421 hydrolysis ⁴⁶, we next subjected the polyP 1,300-mer to non-enzymatic digestion by Mg²⁺, along
422 with Mg²⁺-chelating EDTA to slow down non-enzymatic polyP endo-cleavages. Our data revealed
423 that the length of the polyP products was slightly reduced in a time-dependent manner at 70°C
424 (**Figure 8A**); however, even after 4 hours of incubation, the size of the polyP products was still
425 quite large (and the chain length remained much higher than the polyP 200–500-mer marker).
426 Thus, we decided to increase the reaction temperature to 95°C. Over just one hour, the polyP length
427 was reduced in a time-dependent manner, ultimately reaching a length on the order of 100-mer,
428 while passing through the entire range of polymer lengths between 100–1,300-mer (**Figure 8B**).
429 Moreover, the overall polyP concentration remained greater than 90% after the non-enzymatic
430 hydrolytic process, confirming this process to be efficient with minimal loss of polyP product
431 (**Figure 8C, Table 2**). Thus, polyP mixtures enriched with a narrow length range between 100–
432 1,300-mer can be produced in high yield from the polyP 1,300-mer obtained from our enzymatic
433 method, something hardly achievable with other synthetic polyP methods developed previously.
434 The overall percentage yield of polyP 100-mer via our novel process is ~76%, which is ~2.5 times
435 higher than the reported percentage yield of polyP via the traditional route (~30%), along with a
436 4–7 times lower carbon footprint than the traditional routes (**Table S3**). Therefore, the chemo-
437 enzymatic process developed in this study is also highly “green” based on the green metrics.

438 As mentioned previously, our prior study revealed that PPK2 is more efficient in utilizing
439 a polyP 100-mer than commercial short-chain polyP (25–65-mer) for ATP regeneration (at the
440 same phosphate molar content). Thus, to demonstrate the added value of the non-enzymatic
441 hydrolytic polyP 100-mer product while confirming its activity, we used the polyP 100-mer

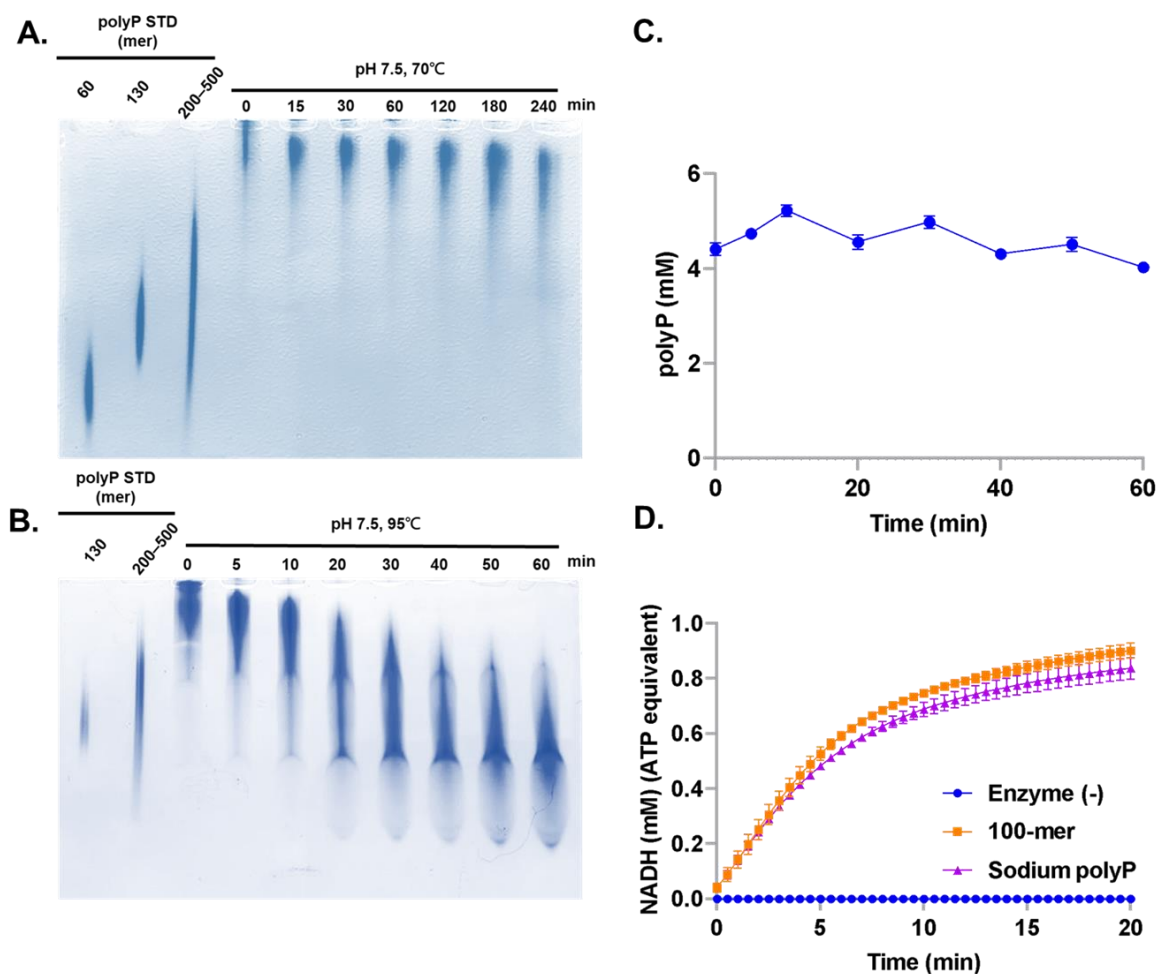
442 product to perform the *Cytophaga* PPK2-based ATP regeneration process. Indeed, we observed
443 more efficient ATP regeneration in the assays using the polyP 100-mer product than those using
444 the commercial short-chain polyP (Figure 8D), suggesting the added value of the produced polyP
445 100-mer. We also note that other than the 100-mer, polyP of other lengths that are non-
446 enzymatically generated from the homogeneous 1,300-mer, especially those between 100-mer and
447 300-mer, could also be used for biomedical applications (Figure 1). Altogether, the entire chemo-
448 enzymatic system presented herein has resulted in a sustainable P bioeconomy platform valorizing
449 low-value biomass waste to produce high-value products.

450

451

452

453



454

455 **Figure 8. Time-dependent thermo-digestion of a homogeneous polyP 1,300-mer by non-**
 456 **enzymatic hydrolysis. (A-B)** The polyP 1,300-mer was incubated at **(A)** 70°C and **(B)** 95°C and
 457 at pH 7.5, along with 5 mM Mg²⁺ and 5 mM ethylenediaminetetraacetic acid. The reaction
 458 mixtures collected at different time points were analyzed by TBE-Urea polyacrylamide gel
 459 electrophoresis, along with commercial polyP standards as a reference for the lengths. **(C)** The
 460 total concentration of polyP (based on the molar content of orthophosphate) during the time-
 461 dependent thermo-digestion was monitored by TBO assay. **(D)** HK-G6PD-mediated **NADPH**
 462 production, which was coupled to *Cytophaga* PPK2-mediated ATP regeneration; commercial
 463 short-chain polyP and purified polyP 100-mer product was the high-energy phosphate donor
 464 (normalized to the same molar content of orthophosphate). Error bars represent the standard
 465 deviation and the data points represent the mean from three independent experimental replicates.

466 Discussion

467 In this study, we devised an efficient enzyme cascade to sustainably produce polyP 1,300-
468 mer from wastewater microalgal biomass (or from commercial short-chain polyP). This
469 technology simultaneously purifies wastewater to avoid eutrophication of downstream aquatic
470 environments (**SDG 6**), while also mitigating the global phosphorus deficit and producing high-
471 value biomedical materials following non-enzymatic hydrolysis (**SDG 3**). From a biochemical
472 standpoint, the success of this technology results from the unusual properties of (i) CK that allow
473 a pH-based modulation of the direction of polyP-ATP phospho-transfer (thermodynamic coupling)
474 and (ii) *Cytophaga PPK2* and *Ralstonia PPK2c* that allow a two-step back-and-forth polyP
475 phospho-transfer. However, this technique also succeeds due to a unique phase-transition property
476 of the polyP reactants and products. In biology, phase transitions have often been employed to
477 circumvent thermodynamic limitations, which can direct and inhibit the reversibility of bio-
478 polymerization reactions to accumulate high concentrations of polymerization products in cells¹⁴,
479 as is also observed in the case of polyP accumulation in the *Chlorella* cells (**Figure 2B**). We thus
480 employed the same principles to drive the enzymatic synthesis of solid long-chain polyP from
481 soluble polydisperse polyP, where the phase-transition of the polyP products from soluble to
482 insoluble leads to the favorability of the forward polyP synthesis process in solution. Moreover,
483 the solidity of the long-chain polyP 1,300-mer products facilitates a streamlined, one-step polyP
484 purification procedure *via* simple filtration for downstream use.

485 The presented microalgal cultivation and extraction procedures at the lab scale also have
486 the potential to be up-scaled to the industrial levels. While microalgal biomass collection,

487 sonication-based cell disruption, and heating seem to be easily scalable, the centrifugation step
488 required for the insoluble microalgal polyP separation from other cell debris could be one hurdle
489 in the development at large scale due to capacity limitations in centrifugal volume. Therefore,
490 future development of techniques that can facilitate both protease/lipase-based cell lysis to allow
491 us to access the microalgal polyP and membrane-based filtration to separate the microalgal polyP
492 from other cell debris at large scale would be required to bring the long-chain polyP synthesis
493 method into the industrial level. Similarly, the bio-enzymatic procedures to convert polydisperse
494 microalgal polyP into insoluble polyP 1,300-mer have currently been designed as a one-pot, two-
495 step cascade at the lab scale. Future optimization that allows the enzymatic conversion process to
496 upscale would be essential to facilitate long-chain polyP at the industrial scale. For example, the
497 use of magnetic nanoparticles to immobilize the His-tagged enzymes could bypass the need for
498 centrifugation and allow enzyme recycling. Moreover, further investigations into a “panacean”
499 buffer system that could accommodate the required catalytic conditions for all the enzymatic
500 components would allow a one-pot process without any loss in yield.

501 Given that the polyP-accumulating *Chlorella* spp. is regarded as Generally Recognized as
502 Safe (GRAS) by the USA Federal Drug Administration (FDA), the value-added polyP products of
503 various lengths reliably produced by our novel procedure could be used in biomedicine. In
504 particular, polyP products of specific lengths can be used in bone stitches (300–1300-mer), as
505 antivirals (100–300-mer), or as drug delivery vessels (10–100-mer). Moreover, future discovery
506 of the unexplored biological functions or medical applications of purified polyP products of
507 lengths greater than 700-mer (other than bone materials) could also result in greater value for our
508 system. Furthermore, the intermediate creatine phosphate synthesized using the microalgal polyP

509 could also be used as medicine for heart failure, cardiac surgery, and skeletal muscle hypertrophy
510 ^{47,48}.

511

512 **Conclusions**

513 Altogether, the catalytic processes established in this study facilitate a sustainable P-
514 bioeconomy platform that can valorize microalgal biomass to produce value-added polyP products
515 at the lab scale. However, a large-scale global sustainable P-bioeconomy is crucial to solving the
516 imminent loss of all global phosphate sources in the next 70 years. Thus, we expect that upon
517 scale-up and further development, the scale of the sustainable P-bioeconomy platform will increase
518 to allow the production of large amounts of high-value polyP materials that are essential for
519 biotechnology and medicine. In particular, as microalgae are abundant in most aquatic ecosystems,
520 an initial application of our polyP synthesis technique in global regions with coasts or rivers that
521 undertake significant phosphorus mineral mining activities would help those regions to divest from
522 economic reliance on phosphorus mineral mining (**SDG 9**). The subsequent establishment of a
523 sustainable P-bioeconomy in other regions lacking phosphorus minerals would help to drive the
524 establishment of local, self-sustainable polyP material production, thereby reducing impacts both
525 of phosphate mineral mining as well as environmental costs related to constant shipping and
526 acquisition of polyP materials.

527

528

529 **Acknowledgments**

530 The authors acknowledge Toshikazu Shiba and other employees of RegeneTiss for providing EX-
531 polyP as standard samples, as well as performing HPLC gel-filtration analysis of the synthesized
532 polyP 1,300-mer. P.-H.W. is supported by the National Science and Technology Council of
533 Taiwan (112-2628-E008-005). T.Z.J. is supported by the Japan Society for the Promotion of
534 Science (JSPS) (Grant-in-aid 21K14746) and the Mizuho Foundation for the Promotion of
535 Science. K.F. is supported by an ELSI research grant and NINS Astrobiology Center grant
536 (AB301003 and AB311001).

537

538 **Author contributions**

539 T.Z.J. and P.-H.W. conceptualized the project and designed experiments. Y.-H.L., S.N., F.-I., Y.,
540 and P.-H.W. performed experiments. All authors contributed to data analysis and interpretation.
541 Y.-H.L., S.N., T.Z.J., and P.-H.W. wrote the manuscript with support from all authors.

542

543 **Declaration of interests**

544 The authors declare no competing interests.

545

546

547

548

549

550

551

552 **References**

553 1 A. A. Yaroshevsky, *Geochemistry International*, **44**, 48–55.

- 554 2 FAO-Food and A. O. of the United Nations, 2017.
- 555 3 Z. Yuan, S. Jiang, H. Sheng, X. Liu, H. Hua, X. Liu and Y. Zhang, *Environmental Science &*
556 *Technology*, 2018, **52**, 2438–2450.
- 557 4 R. Noyes, .
- 558 5 Y. Liu, G. Villalba, R. U. Ayres and H. Schroder, *Journal of Industrial Ecology*, 2008, **12**,
559 229–247.
- 560 6 D. W. Schindler, R. E. Hecky, D. L. Findlay, M. P. Stainton, B. R. Parker, M. J. Paterson, K.
561 G. Beaty, M. Lyng and S. E. M. Kasian, *Proceedings of the National Academy of Sciences of*
562 *the United States of America*, 2008, **105**, 11254–11258.
- 563 7 E. Martin, J. Lalley, W. Wang, M. N. Nadagouda, E. Sahle-Demessie and S.-R. Chae,
564 *Chemical Engineering Journal*, 2018, **352**, 612–624.
- 565 8 S. Chae, B. Murugesan, H. Kim, D. K. Duvvuru, T. Lee, Y.-H. Choi, M.-H. Baek and M. N.
566 Nadagouda, *ACS ES T Water*, 2021, **1**, 1657–1664.
- 567 9 Z. Yuan, S. Pratt and D. J. Batstone, *Current Opinion in Biotechnology*, 2012, **23**, 878–883.
- 568 10 A. T. Nielsen, W. T. Liu, C. Filipe, L. Grady Jr, S. Molin and D. A. Stahl, *Applied and*
569 *Environmental Microbiology*, 1999, **65**, 1251–1258.
- 570 11 L. Wang, M. Min, Y. Li, P. Chen, Y. Chen, Y. Liu, Y. Wang and R. Ruan, *Applied*
571 *Biochemistry and Biotechnology*, 2010, **162**, 1174–1186.
- 572 12 A. Lavrinovičs, L. Mežule and T. Juhna, *Algal Research*, 2020, **52**, 102090.
- 573 13 S. Eixler, U. Selig and U. Karsten, *Hydrobiologia*, 2005, **533**, 135–143.
- 574 14 E. Bondy-Chorney, I. Abramchuk, R. Nasser, C. Holinier, A. Denoncourt, K. Bajjal, L.
575 McCarthy, M. Khacho, M. Lavallée-Adam and M. Downey, *Cell Reports*, 2020, **33**, 108318.
- 576 15 W. E. G. Müller, H. C. Schröder and X. Wang, *Chemical Reviews*, 2019, **119**, 12337–12374.
- 577 16 W. E. G. Müller, E. Tolba, H. C. Schröder and X. Wang, *Macromolecular Bioscience*, 2015,
578 **15**, 1182–1197.
- 579 17 W. E. G. Müller, H. Schepler, M. Neufurth, S. Wang, V. Ferrucci, M. Zollo, R. Tan, H. C.
580 Schröder and X. Wang, *Journal of Materials Science and Technology*, 2023, **135**, 170–185.
- 581 18 H. Schepler, M. Neufurth, S. Wang, Z. She, H. C. Schröder, X. Wang and W. E. G. Müller,
582 *Theranostics*, 2022, **12**, 18–34.
- 583 19 P. Dinarvand, S. M. Hassanian, S. H. Qureshi, C. Manithody, J. C. Eissenberg, L. Yang and
584 A. R. Rezaie, *Blood*, 2014, **123**, 935–945.

- 585 20 J. H. Morrissey, S. H. Choi and S. A. Smith, *Blood*, 2012, **119**, 5972–5979.
- 586 21 B. Lorenz, J. Münkner, M. P. Oliveira, A. Kuusksalu, J. M. Leitão, W. E. Müller and H. C.
587 Schröder, *Biochimica et Biophysica Acta*, 1997, **1335**, 51–60.
- 588 22 J. Roewe, G. Stavrides, M. Strueve, A. Sharma, F. Marini, A. Mann, S. A. Smith, Z. Kaya,
589 B. Strobl, M. Mueller, C. Reinhardt, J. H. Morrissey and M. Bosmann, *Nature*
590 *Communications*, 2020, **11**, 4035.
- 591 23 V. Ferrucci, D.-Y. Kong, F. Asadzadeh, L. Marrone, A. Boccia, R. Siciliano, G. Criscuolo,
592 C. Anastasio, F. Quarantelli, M. Comegna, I. Pisano, M. Passariello, I. Iacobucci, R. D.
593 Monica, B. Izzo, P. Cerino, G. Fusco, M. Viscardi, S. Brandi, B. M. Pierri, G. Borriello, C.
594 Tiberio, L. Atripaldi, M. Bianchi, G. Paoletta, E. Capoluongo, G. Castaldo, L. Chiariotti, M.
595 Monti, C. De Lorenzo, K.-S. Yun, S. Pascarella, J.-H. Cheong, H.-Y. Kim and M. Zollo,
596 *Science signaling*, 2021, **14**, eabe5040.
- 597 24 T. Z. Jia, P.-H. Wang, T. Niwa and I. Mamajanov, *Journal of Biosciences*, 2021, **46**, 79.
- 598 25 M. J. Gray, W.-Y. Wholey, N. O. Wagner, C. M. Cremers, A. Mueller-Schickert, N. T. Hock,
599 A. G. Krieger, E. M. Smith, R. A. Bender, J. C. A. Bardwell and U. Jakob, *Molecular Cell*,
600 2014, **53**, 689–699.
- 601 26 M. Nakagaki, H. Inoue, T. Fujie and S. Ohashi, *BCSJ*, 1963, **36**, 595–599.
- 602 27 A. Momeni and M. J. Filiaggi, *Journal of Non-Crystalline Solids*, 2013, **382**, 11–17.
- 603 28 D. Wang, Y. Li, H. A. Cope, X. Li, P. He, C. Liu, G. Li, S. M. Rahman, N. B. Tooker, C. B.
604 Bott, A. Onnis-Hayden, J. Singh, A. Elfick, R. Marques, H. J. Jessen, A. Oehmen and A. Z.
605 Gu, *Water Research*, 2021, **206**, 117726.
- 606 29 L. Achbergerová and J. Nahálka, *Microbial Cell Factories*, 2011, **10**, 63.
- 607 30 K. Motomura, R. Hirota, M. Okada, T. Ikeda, T. Ishida and A. Kuroda, *Applied and*
608 *Environmental Microbiology*, 2014, **80**, 2602–2608.
- 609 31 A. E. Parnell, S. Mordhorst, F. Kemper, M. Giurrandino, J. P. Prince, N. J. Schwarzer, A.
610 Hofer, D. Wohlwend, H. J. Jessen, S. Gerhardt, O. Einsle, P. C. F. Oyston, J. N. Andexer and
611 P. L. Roach, *Proceedings of the National Academy of Sciences of the United States of*
612 *America*, 2018, **115**, 3350–3355.
- 613 32 B. P. Nocek, A. N. Khusnutdinova, M. Ruszkowski, R. Flick, M. Burda, K. Batyrova, G.
614 Brown, A. Mucha, A. Joachimiak, Ł. Berlicki and A. F. Yakunin, *ACS Catalysis*, 2018, **8**,
615 10746–10760.

- 616 33 E. Kozaeva, M. Nieto-Domínguez, A. D. Hernández and P. I. Nickel, *RSC Chemical Biology*,
617 2022, **3**, 1331–1341.
- 618 34 M. Tavanti, J. Hosford, R. C. Lloyd and M. J. B. Brown, *Green Chemistry*, 2021, **23**, 828–
619 837.
- 620 35 J. C. Hildenbrand, G. A. Sprenger, A. Teleki, R. Takors and D. Jendrossek, *Microbial*
621 *Physiology*, 2022, **33**, 1–11.
- 622 36 S. Mordhorst, J. Siegrist, M. Müller, M. Richter and J. N. Andexer, *Angewandte Chemie*
623 *International Edition in English*, 2017, **56**, 4037–4041.
- 624 37 P.-H. Wang, K. Fujishima, S. Berhanu, Y. Kuruma, T. Z. Jia, A. N. Khusnutdinova, A. F.
625 Yakunin and S. E. McGlynn, *ACS Synthetic Biology*, 2020, **9**, 36–42.
- 626 38 J. C. Hildenbrand, A. Teleki and D. Jendrossek, *Applied Microbiology and Biotechnology*,
627 2020, **104**, 6659–6667.
- 628 39 T. Tumlirsch, A. Sznajder and D. Jendrossek, *Applied and Environmental Microbiology*,
629 2015, **81**, 8277–8293.
- 630 40 C. Mukherjee, C. Mukherjee and K. Ray, *Protoc. Exch.*, , DOI:10.1038/protex.2015.067.
- 631 41 R. Ohtomo, Y. Sekiguchi, T. Mimura, M. Saito and T. Ezawa, *Analytical Biochemistry*, 2004,
632 **328**, 139–146.
- 633 42 S. Daliry, A. Hallajisani, J. Mohammadi Roshandeh, H. Nouri and A. Golzary, *Global*
634 *Journal of Environmental Science and Management*, 2017, **3**, 217–230.
- 635 43 F.-F. Chu, P.-N. Chu, P.-J. Cai, W.-W. Li, P. K. S. Lam and R. J. Zeng, *Bioresource*
636 *Technology*, 2013, **134**, 341–346.
- 637 44 *J. Biol. Chem.*, 1973, **248**, 4803–4810.
- 638 45 D. G. Bolesch and J. D. Keasling, *Journal of Biological Chemistry*, 2000, **275**, 33814–33819.
- 639 46 N. H. Williams, *Journal of the American Chemical Society*, 2000, **122**, 12023–12024.
- 640 47 E. Strumia, F. Pelliccia and G. D'Ambrosio, *Advances in Therapy*, 2012, **29**, 99–123.
- 641 48 D. L. Horjus, I. Oudman, G. A. van Montfrans and L. M. Brewster, *Cochrane database of*
642 *systematic reviews*, 2011, CD005184.

643 **Tables**

644 **Table 1. eQuilibrator-based estimation of the Gibbs free energy (Δ_rG^m) of the listed**
 645 **enzymatic reactions under the following experimental conditions: 1 mM reactant**
 646 **concentration, pH 7.5, 25°C, pMg 3.0, and 0.25 M ionic strength).**
 647

| | Reaction | Δ_rG^m (kJ/mol) |
|--------|---|------------------------|
| I | $\text{PolyP}_{(n)} + \text{ATP} \rightarrow \text{PolyP}_{(n+1)} + \text{ADP}$ | ~0 |
| II | $\text{ADP} + \text{Creatine phosphate} \rightarrow \text{ATP} + \text{Creatine}$ | -12.2 |
| I + II | $\text{PolyP}_{(n)} + \text{Creatine phosphate} \rightarrow \text{PolyP}_{(n+1)} + \text{Creatine}$ | -12.2 |

648
 649
 650
 651
 652
 653
 654
 655
 656
 657
 658
 659
 660
 661
 662
 663
 664
 665
 666
 667

668 **Table 2. The output summary of each step of the one-pot, two-step polyphosphate**
 669 **(polyP) synthesis**

| Step | Substrates | Products | Yield (%) | Residues and Byproducts | Residual polyP yield (%) |
|--|----------------------------|--------------------------------------|------------------|------------------------------------|---------------------------------|
| A. Synthesis of creatine phosphate from microalgal polyP | Algal polyP, Creatine | Creatine phosphate | 95% | Creatine, Algal polyP (< 5-mer) | 95% |
| B. Enzyme removal/pH adjustment | N.A. | N.A. | 99% | N.A. | 94% |
| C. Synthesis of long-chain polyP | Creatine phosphate, ATP | Insoluble long-chain polyP 1,300-mer | 90% | Creatine | 84.6% |
| D. Filtration | N.A. | N.A. | 99% | N.A. | 84% |
| E. Hydrolysis of long-chain polyP | Long-chain polyP 1,300-mer | polyP 100–1,300-mer | 90% | P _i | 75.5% |